

Thermal radiation and chemical reaction effect on Casson Fluid, Heat and Mass Transfer over a Permeable Vertical Stretching Surface

¹Y. Hari Krishna, ²P. Bindu

ABSTRACT: *This article studies Casson fluid flow, heat and mass transfer over a permeable vertical stretching surface considering the effects of magnetic field, thermal radiation and chemical reaction. After applying the suitable similarity transforms the governing equations of flow are solved numerically by shooting technique along with 6th order Runge-Kutta iteration scheme with MATLAB package. The impacts of various values of parameters on the velocity, temperature and concentration distributions are discussed through graphs. Expressions for shear stress, rate of heat transfer and rate of mass transfer are analysed and given in tabular form.*

Keywords: *Casson fluid, Prandtl number, Bouncy parameter, Heat transfer and Mass transfer*

I. INTRODUCTION

Analysis of Casson fluid flow, heat transfer and mass transfer in two-dimensional (2-D) boundary layers over a porous stretching surface has attracted attentions of many scholars. In processes such situations occur in many cooling of metallic plates, rolling, manufacturing of food etc. The objective of this research on Casson fluid flow, heat and mass transfer over permeable stretching sheet in presence of radiation and chemical reaction effect.

Eldabe *et al.* [1] discussed between two rotating cylinders of Non-Newtonian Casson fluid flow. Nadeem *et al.*[2] presented MHD Casson fluid flow over an exponentially shrinking sheet. Hayat *et al.*[3] have studied MHD Casson fluid flow with respect to Soret and Dufour effects. Pramanik [4] studied Casson fluid flow and heat transfer past an exponentially porous stretching surface. M. Gnaneswara Reddy [5] analysed Casson fluid of unsteady radiative-convective boundary layer flow in presence of thermal conductivity. Khalid *et al.*[6] discussed unsteady MHD Casson flow. Akbar [7] depicts Casson fluid of peristaltic flow in presence of magnetic field effect. Khalid *et al.*[8] illustrated MHD Casson free convection flow. Raju *et al.*[9] discussed MHD Casson fluid flow in heat transfer and mass transfer. Bala [10] presented MHD Casson fluid flow over an exponentially inclined permeable stretching surface. Raju *et al.*[11] analysed MHD of heat and mass transfer in Casson fluid flow over an exponentially permeable stretching surface. Reddy *et al.* [12] discussed MHD flow along a moving vertical plate in presence of jouble heating effect. Reddy [13] studied MHD flow past a vertical porous plate in presence of Soret and Dufour effect. Mangathai *et al.*[14] illustrated MHD flow past a vertical

¹ Dept of Mathematics, ANURAG Engineering College, Ananthagiri, Kodad, Telangana, India-508206

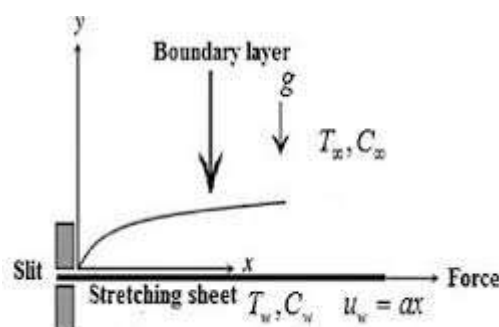
² Department of Mathematics, Koneru Lakshmaiah Education Foundation, Vaddeswaram, Guntur, AP, India- 522 502

porous plate. Ramana *et al.*[15] discussed effect of radiation and chemical reaction of MHD oscillatory flow over a vertical surface in a porous. Ramana Reddy *et al.*[16] discussed MHD flow along a moving vertical porous plate in presence of radiation and chemical reaction effect. Very recently, the researchers [17-27] illustrated the heat and mass transfer behaviour of MHD Casson flows by considering stretching surface.

From the above studies, we say that little work has been made to analysis the Casson fluid flow considering thermal radiation and chemical reaction. The objective of the work is to study the Casson fluid flow and heat and mass transfer over a permeable vertical surface in presence of magnetic field , thermal radiation and chemical reaction effects numerically by shooting method. The effects of different involved parameter on the fluid velocity, temperature and concentration profiles along with shear stress, heat and mass transfer rates has been discussed through graphically and tabular forms.

II. MATHEMATICAL FORMULATION

Consider a steady 2-D boundary layer flow the effect of heat generation, thermal radiation and chemical reaction on viscous incompressible electrically conducting fluid along a permeable vertical stretching sheet. Two equal and opposite forces are introduced along the x-axis so that the sheet is stretched keeping the origin fixed as seen in Figure 1. A magnetic field B_0 of uniform strength is applied in y-direction. In comparison to the applied magnetic field in presence of magnetic field effect is neglected. Here x-axis is considered along the direction of the plate and y-axis is taken normal to it.



Then the equation of state for an isotropic flow of a Casson fluid is [1]

$$\tau_{ij} = 2 \left(\mu_b + \frac{P_y}{\sqrt{2\pi}} \right) e_{ij}$$

(1)

Where e_{ij} is the $(i, j)^{th}$ component of deformation rate, τ_{ij} is the $(i, j)^{th}$ component of the stress tensor, π is the product of the component of deformation rate with itself, and μ_b is the plastic dynamic viscosity. The yield stress P_y is expressed as, $P_y = \frac{\mu b \sqrt{2\pi}}{\beta}$ where β Casson fluid parameter. For non-Newtonian Casson fluid

flow $\mu = \mu_b + \frac{P_y}{\sqrt{2\pi}}$ which gives $\nu' = \nu \left(1 + \frac{1}{\beta} \right)$, where $\nu = \frac{\mu b}{\rho}$ is viscosity. It is assumed that plate

temperature is initially T_w , while the temperature far away the sheet is T_∞ . If u is velocity component in x - directions and v is also the velocity component in y -directions.

the boundary layer flow of Casson fluid are governs as following equations,

$$\frac{\partial u}{\partial x} + \frac{\partial v}{\partial y} = 0 \tag{2}$$

$$u \frac{\partial u}{\partial x} + v \frac{\partial u}{\partial y} = \nu \left(1 + \frac{1}{\beta} \right) \frac{\partial^2 u}{\partial y^2} + g_0 \beta^* (T - T_\infty) - \frac{\sigma B_0^2}{\rho} u \tag{3}$$

$$u \frac{\partial T}{\partial x} + v \frac{\partial T}{\partial y} = \frac{k}{\rho c_p} \frac{\partial^2 T}{\partial y^2} + \frac{Q_0}{\rho c_p} (T - T_\infty) - \frac{1}{\rho c_p} \frac{\partial q_r}{\partial y} \tag{4}$$

$$u \frac{\partial C}{\partial x} + v \frac{\partial C}{\partial y} = D_m \frac{\partial^2 C}{\partial y^2} - Kr(C - C_\infty) \tag{5}$$

where g_0 is the acceleration due to gravity, β^* is the volumetric co-efficient of thermal expansion, σ is the electric conductivity, B_0 is the uniform magnetic field strength, ρ is the fluid density, c_p is the specific heat at constant pressure, k is the thermal conductivity, Q_0 is the volumetric rate of heat generation and q_r is the radiative heat flux. D_m is the coefficient of the mass diffusivity, C is the concentration of the fluid, Kr is the chemical reaction parameter,

The corresponding boundary conditions are

$$\left. \begin{aligned} u = u_w, v = v_w(x), \quad T = T_w, C = C_w \quad \text{at } y = 0 \\ u = 0, \quad T = T_\infty, C = C_\infty \quad \text{as } y \rightarrow \infty \end{aligned} \right\} \tag{6}$$

where u_w is the tangential velocity and we consider $u_w = Dx, D(>0)$ is a constant and v_w is the suction velocity.

Using Rosseland approximation for radiation we can get

$$q_r = -\frac{4\sigma^*}{3k'} \frac{\partial T^4}{\partial y} \tag{7}$$

where σ^* is the Stefan- Boltzman constant and $3k'$ is the absorption coefficient. Here we consider the temperature difference within the flow is very small such that T^4 may be expanded as a linear function of temperature. Using Taylor series and neglecting the higher order terms, we get, $T^4 \cong 4T_\infty^3 T - 3T_\infty^4$. Thus equation (4) implies

$$u \frac{\partial T}{\partial x} + v \frac{\partial T}{\partial y} = \frac{k}{\rho c_p} \frac{\partial^2 T}{\partial y^2} + \frac{Q_0}{\rho c_p} (T - T_\infty) + \frac{16\sigma^* T_\infty^3}{3k' \rho c_p} \frac{\partial^2 T}{\partial y^2} \quad (8)$$

Equations (3) to (8) can be made dimensionless quantities by introducing the following change of variables

$$u = Dxf'(\eta), v = -\sqrt{Dg}f(\eta) = y\sqrt{\frac{D}{g}}, \psi = \sqrt{Dg}xf(\eta), \theta(\eta) = \frac{T - T_\infty}{T_w - T_\infty}, \phi(\eta) = \frac{C - C_\infty}{C_w - C_\infty} \quad (9)$$

where ψ is called the stream function, the dimensionless distance normal to the sheet is denoted by η , θ and ϕ are said that the dimensionless temperature, concentration respectively.

Using equation (9) in equations (3) and (8), we get

$$\left(1 + \frac{1}{\beta}\right) f''' + ff'' - f'^2 + \gamma\theta - Mf' = 0 \quad (10)$$

$$\left(1 + \frac{4}{3}N\right) \theta'' + Pr f \theta' + Pr Q\theta = 0 \quad (11)$$

$$\phi'' + NSc(4f'\phi - f\phi') - ScKr\phi = 0 \quad (12)$$

The reduced boundary conditions are

$$\left. \begin{aligned} f' = 1, \quad f = f_w, \quad \theta = 1, \phi = 1 \quad \text{at } \eta = 0 \\ f' = 0, \quad \theta = 0, \phi = 0 \quad \text{as } \eta \rightarrow \infty \end{aligned} \right\} \quad (13)$$

where $M = \frac{\sigma B_0^2}{\rho D}$ is the magnetic field parameter, $\gamma = \frac{g\beta_T(T_w - T_\infty)}{D^2 x}$ is the buoyancy parameter,

$Q = \frac{Q_0}{D\rho c_p}$ is the heat source parameter, $Pr = \frac{\mu c_p}{k}$ is the Prandtl number, $Ec = \frac{D^2 x^2}{c_p(T_w - T_\infty)}$ is the Eckert

number, $f_w = -\frac{v_w}{\sqrt{Dg}}$ is the suction parameter and $N = \frac{4\sigma^* T_\infty^3}{kk'}$ is the radiation parameter. $Sc = \frac{\nu_f}{D_m}$ is the

Schmidt number, $Kr = \frac{K_0 L}{C_0 U_0}$ is the chemical reaction

Finally, skin friction coefficient (C_f), local Nusselt number (Nu_x) and Sherwood number (Re_x) can be written as

$$Re_x^{\frac{1}{2}} C_f = \left(1 + \frac{1}{\beta}\right) f''(0), Nu_x / Re_x^{\frac{1}{2}} = -\theta'(0), Sh_x Re_x^{-1/2} = -\phi'(0)$$

III. NUMERICAL SOLUTION

The system non-linear differential equations (10)-(12) with the boundary conditions (13) have been solved numerically by shooting technique along with 6th order Runge-Kutta iteration scheme with MATLAB package. The step size is $\Delta\eta = 0.01$ chose to satisfy the convergence criterion of 0.000001 in all cases. The value of η_∞ was found to each iteration loop by $\eta_\infty = \eta_\infty + \Delta\eta$. The maximum value of η_∞ to each group of parameters β, fw, QM, Pr and N determined when the value of the unknown boundary conditions at $\eta = 0$ not change to successful loop with error less than 10^{-6}

IV. Results and Discussion:

The results are showing the nature of the effects of the parameters like $\beta, \gamma, M, N, Pr, Q, Sc$ and Kr are Casson parameter, Bouncy parameter, Magnetic parameter, thermal radiation parameter, Prandtl number, Heat source parameter, Schmidt number chemical reaction parameter respectively, on velocity, temperature and concentration profiles are displayed with help of graphical illustration. Also the shear stress, Nusselt number and Sherwood number are studied and given in table form. We've taken common values of $\beta=1; \gamma=1; M=0.5; N=0.2; Pr=0.71; Q=0.5; Sc=0.6; Kr=0.5; w=0.5$; in respective figures and table.

Figure 2 show the plot of the influence of Casson parameter on velocity profile. It is observed that the velocity decreases when Casson increases. In practice, increasing results in an increase in the plastic dynamic viscosity that produces a resistance in the flow and decrease in fluid velocity thereof. In Figure 3, velocity increases with increasing values of Bouncy parameter (γ). Figure 4 shows that the decrease values of velocity for higher intensities of the M . This is in traditional values with the fact that Lorentz force develops, generate as a result of upper magnetic field strength, and heavily opposes the fluid motion. Figure 5-7 shows that impacts of varying thermal radiation parameter N on velocity, temperature and concentration flows. Here we study that the N increasing convective flow in such a way that velocity increases with the increasing values of N . N enhance temperature profile as thermal boundary layer thickness increase with increasing of N . the temperature distribution is enhanced with an increase in the N . Increasing values of N provide more heat to working fluid, which results in an enticement in the temperature and thermal boundary layer thickness. Effect of N on the concentration, we observed that increase values of N concentration decreases. From Figures 8-10, it is demonstrates the effect of the Prandtl number (Pr) on the velocity, temperature and concentration profiles. It is observed that the velocity, temperature and concentration profiles of the flow decreases as the Pr increases. Fig 8 reveals the effects of Pr on the transient velocity profiles. It is evident from the figure that the velocity decreases with an increase in Pr . In Figure (11) illustrated temperature profiles against η for some representative values of the heat source parameter $Q = 0.2, 0.5, 0.7, 0.9$. The positive value of Q represents source i.e. heat generation in the fluid. We know that when heat is generated the buoyancy force increases, which induces the flow rate to increase, giving rise to decrease in the temperature profiles. Figure 12 depicts the concentration profile for the different values of Schmidt number Sc . We've observed that the Sc increases, the flow concentration decrease across the boundary layer region, a higher Sc implies a lower Brownian diffusion coefficient, which will give rise to a shorter penetration depth for concentration boundary layer.

Figure 13 illustrates the influence of the non-dimensional chemical reaction parameter (Kr) on the concentration profile flow. It can be observed that concentration profiles of the fluid decrease with increasing values of the Kr , because of in Kr speed up the rate of the reactants on the flow and consequently reduces the concentration distribution of the reacting species.

Table 1 shows the numerical values of the Skin friction number, the local Nusselt number and Sherwood number for the parameters β , γ , M , N , Pr , Q , Sc and Kr . We observe that Skin friction number at sheet decrease upon increasing values of all parameter, the values of the local Nusselt number at sheet increase upon increasing values of all parameters and also conclude that the values of Sherwood number decrease upon increasing M , N and Pr , but increase upon increasing β , γ , Q , Sc and Kr .

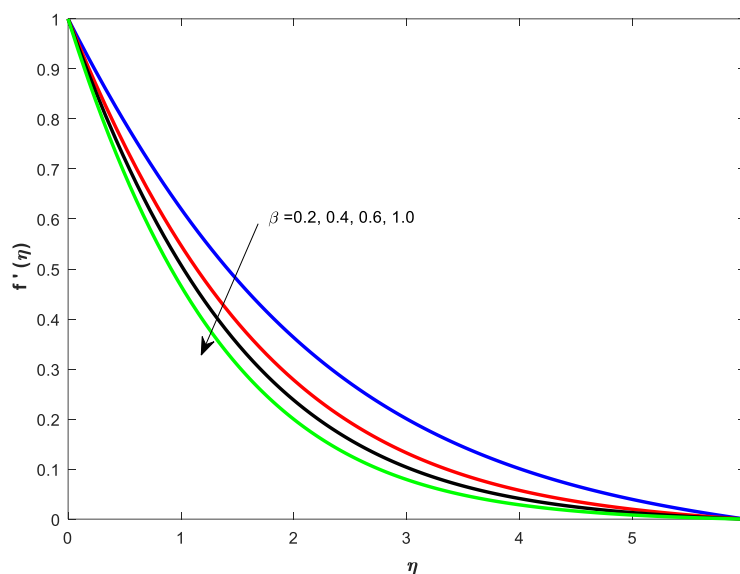


Figure 2: Dominance of B on Velocity

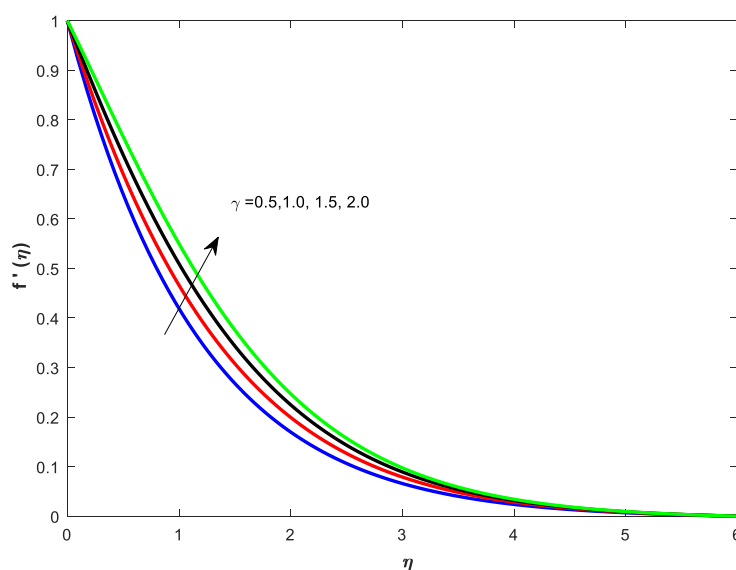


Figure 3: Dominance of γ on Velocity

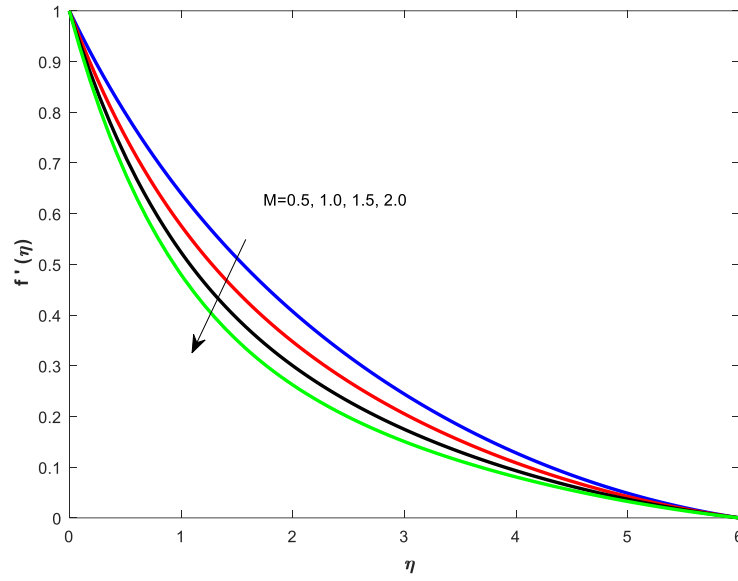


Figure 4: Dominance of M on Velocity

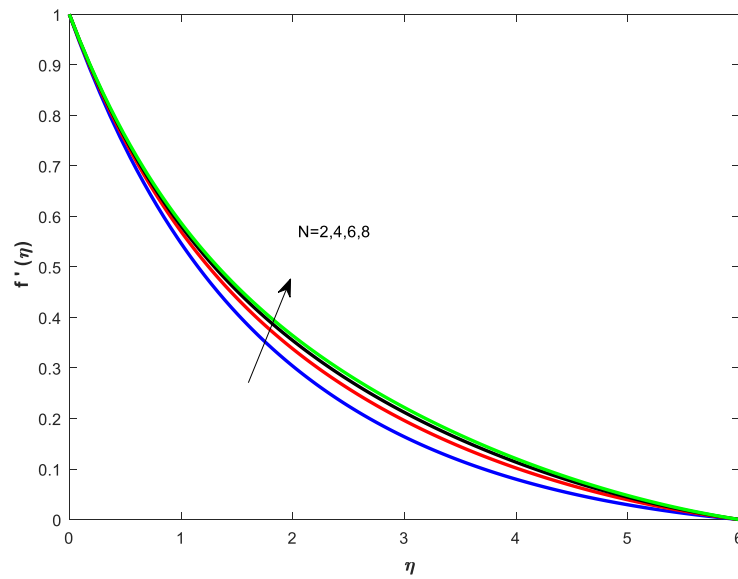


Figure 5: Dominance of N on Velocity

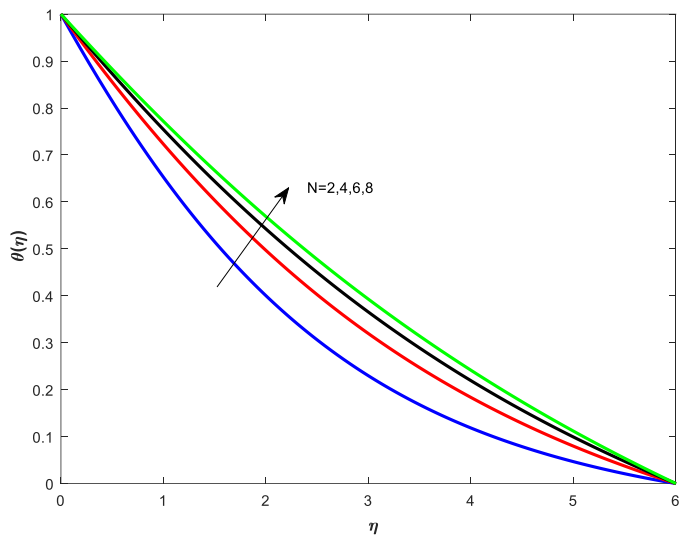


Figure 6: Dominance of N on Temperature

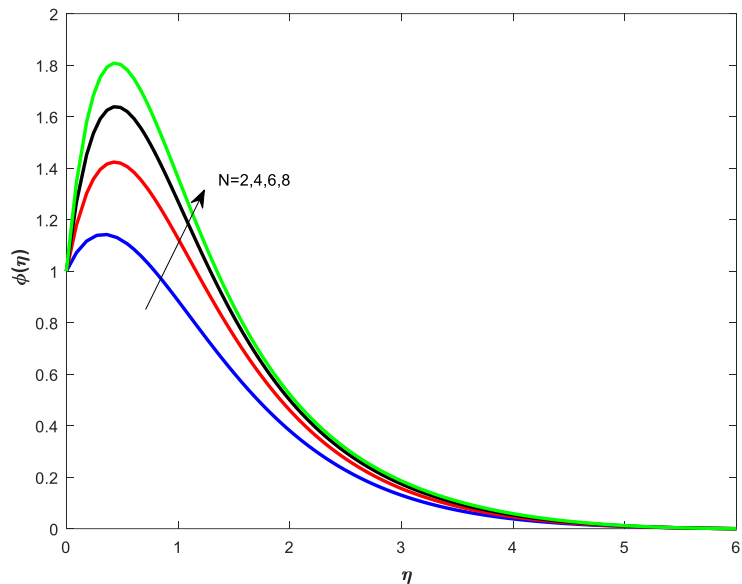


Figure 7: Dominance of N on Concentration

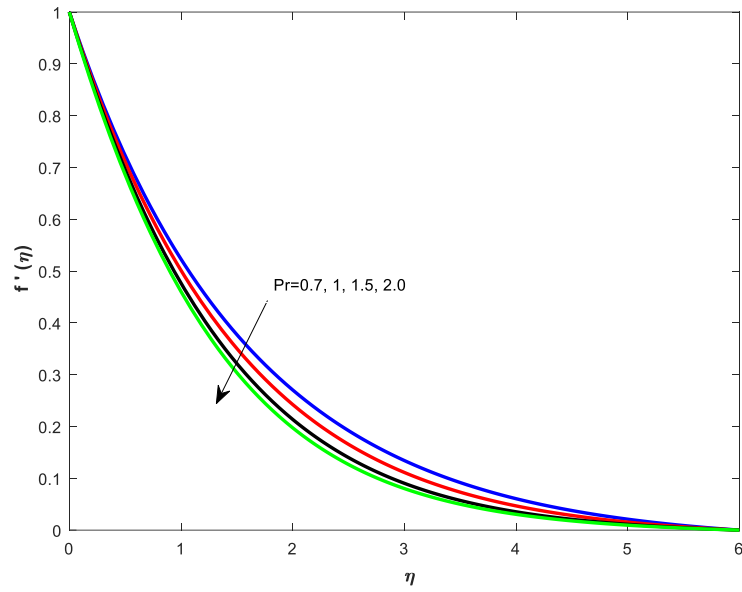


Figure 8: Dominance of Pr on Velocity

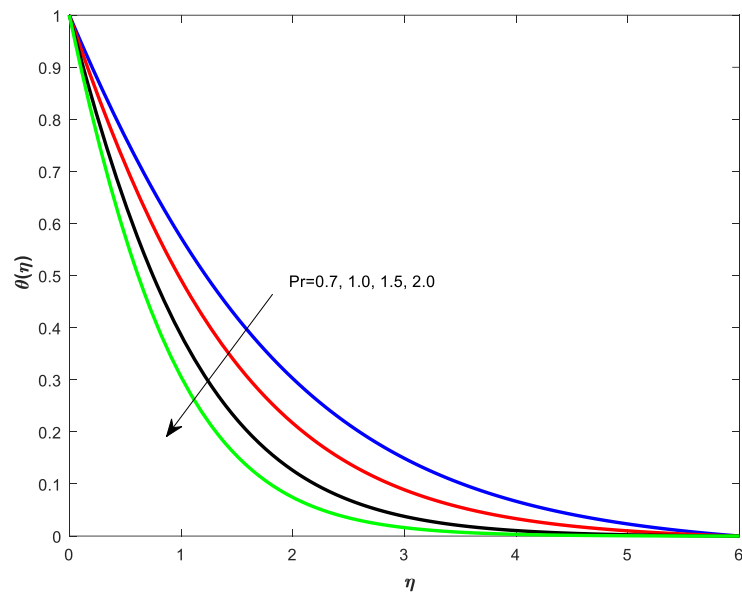


Figure 9: Dominance of Pr on Temperature

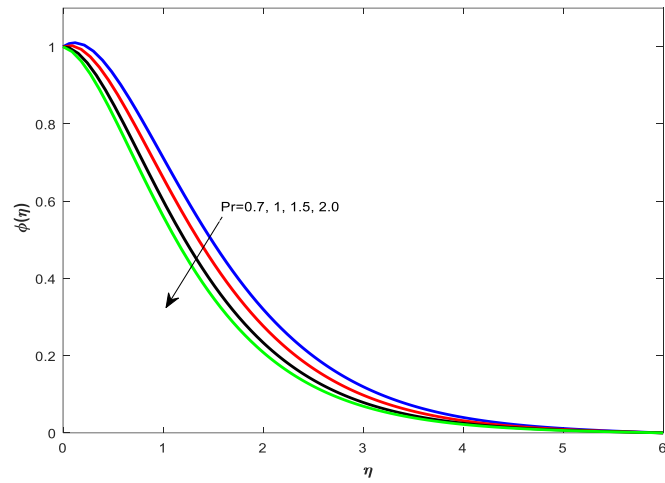


Figure 10: Dominance of Pr on Concentration

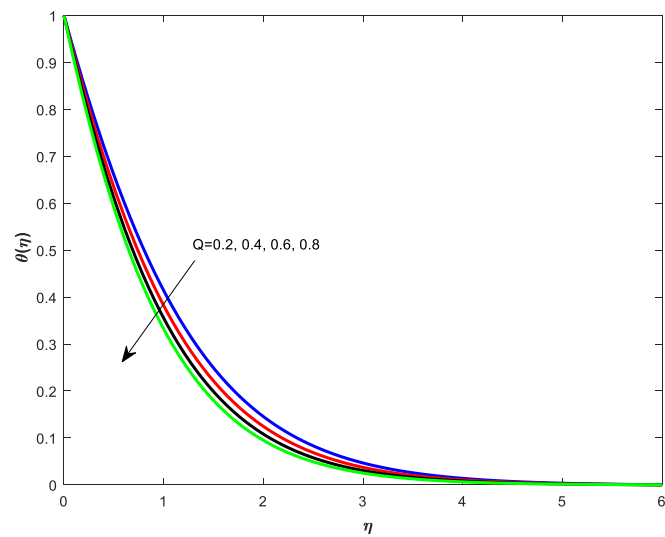


Figure 11: Dominance of Q on Temperature

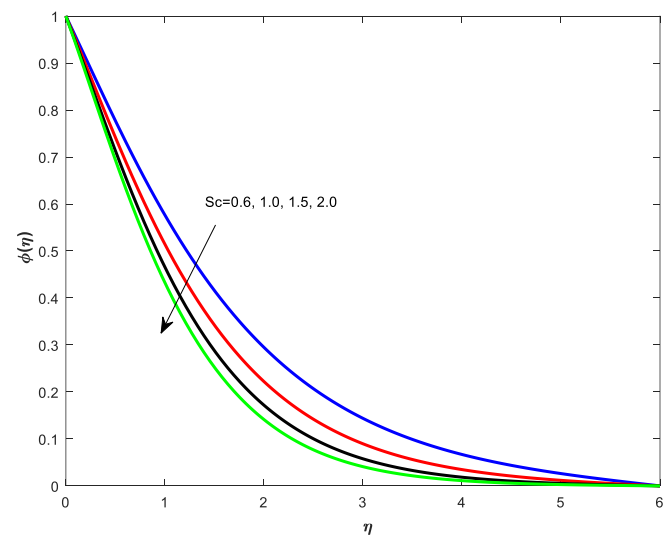


Figure 12: Dominance of Sc on Concentration

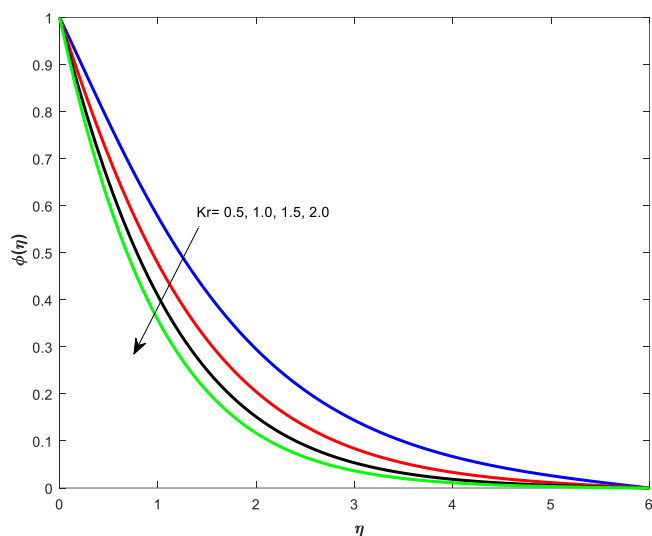


Figure 13: Dominance of Kr on Concentration.

Table 1: Numerical values of the Skin-friction coefficients, Nusselt and Sherwood number

β	γ	M	N	Pr	Q	Sc	Kr	$f''(0)$	$-\theta'(0)$	$-\phi'(0)$
0.2	1	0.5	0.2	0.71	0.5	0.6	0.5	-0.442712	0.877589	0.430424
0.4	1	0.5	0.2	0.71	0.5	0.6	0.5	-0.559855	0.885138	0.436545
0.6	1	0.5	0.2	0.71	0.5	0.6	0.5	-0.631686	0.892002	0.440164
1	1	0.5	0.2	0.71	0.5	0.6	0.5	-0.718533	0.904300	0.444333
1	0.5	0.5	0.2	0.71	0.5	0.6	0.5	-0.455344	0.868515	0.434723
1	1	0.5	0.2	0.71	0.5	0.6	0.5	-0.585047	0.877589	0.439333
1	1.5	0.5	0.2	0.71	0.5	0.6	0.5	-0.718533	0.885905	0.444333
1	2	0.5	0.2	0.71	0.5	0.6	0.5	-0.856576	0.893616	0.449823
1	1	0.5	0.2	0.71	0.5	0.6	0.5	-0.456714	0.270398	-2.680454
1	1	1	0.2	0.71	0.5	0.6	0.5	-0.588389	0.273374	-2.793934
1	1	1.5	0.2	0.71	0.5	0.6	0.5	-0.704749	0.276955	-2.923068
1	1	2	0.2	0.71	0.5	0.6	0.5	-0.809199	0.281322	-3.071725

1	1	0.5	2	0.71	0.5	0.6	0.5	-0.575796	0.239586	-0.961748
1	1	0.5	4	0.71	0.5	0.6	0.5	-0.583055	0.260879	-2.322745
1	1	0.5	6	0.71	0.5	0.6	0.5	-0.595693	0.299598	-3.483852
1	1	0.5	8	0.71	0.5	0.6	0.5	-0.622960	0.391533	-4.513974
1	1	0.5	0.2	0.7	0.5	0.6	0.5	-0.651736	0.504790	-0.007502
1	1	0.5	0.2	1	0.5	0.6	0.5	-0.678748	0.632763	0.065699
1	1	0.5	0.2	1.5	0.5	0.6	0.5	-0.711164	0.829178	-0.106456
1	1	0.5	0.2	2	0.5	0.6	0.5	-0.733853	1.010385	-0.186415
1	1	0.5	0.2	0.71	0.2	0.6	0.5	-0.584841	0.768036	0.426384
1	1	0.5	0.2	0.71	0.4	0.6	0.5	-0.595007	0.850199	0.434866
1	1	0.5	0.2	0.71	0.6	0.6	0.5	-0.603487	0.924377	0.441952
1	1	0.5	0.2	0.71	0.8	0.6	0.5	-0.610723	0.992419	0.448020
1	1	0.5	0.2	0.71	0.5	0.6	0.5	-0.599426	0.888153	0.438556
1	1	0.5	0.2	0.71	0.5	1	0.5	-0.599426	0.888153	0.502789
1	1	0.5	0.2	0.71	0.5	1.5	0.5	-0.599426	0.888153	0.550560
1	1	0.5	0.2	0.71	0.5	2	0.5	-0.599426	0.888153	0.580453
1	1	0.5	0.2	0.71	0.5	0.6	0.5	-0.599426	0.888153	0.438556
1	1	0.5	0.2	0.71	0.5	0.6	1	-0.599426	0.888153	0.648593
1	1	0.5	0.2	0.71	0.5	0.6	1.5	-0.599426	0.888153	0.819151
1	1	0.5	0.2	0.71	0.5	0.6	2	-0.599426	0.888153	0.965997

V. Conclusion:

This study presented the flow, heat and mass transfer behaviour of Casson fluid over a permeable vertical stretching surface considering the effects of magnetic field and thermal radiation and chemical reaction. The conclusions are as follows:

1. Velocity decreases for increasing values of Casson parameter, magnetic parameter M , Prandtl number where as it shows reverse tendency in the case of bouncy parameter and thermal radiation parameter N .
2. Temperature distribution decreases with an increase in Prandtl number Pr and heat Source parameter Q where as it shows reverse tendency in the case of thermal radiation parameter N .
3. Concentration boundary layer decreases with an increase in Prandtl number Pr , chemical reaction Kr and Schmidt number Sc where as it shows reverse tendency in the case of thermal radiation parameter N .

References:

1. Eldabe, N. T. M., Saddeck, G. & El-Sayed, A. F. [2001] "Heat transfer of MHD non-Newtonian Casson fluid flow between two rotating cylinders", *Mechanics and Mechanical Engineering*, Vol. 5, Issue. 2, pp. 237-251.
2. Nadeem, S., Haq, R. U., & Lee, C.[2012] "MHD flow of a Casson fluid over an exponentially shrinking sheet," *Scientia Iranica*, Vol. 19, Issue. 6, pp.1550-1553.
3. T. Hayat, S.A. Shehzad, A. Alsaedi, Soret and Dufour effects on magnetohydrodynamic (MHD) flow of Casson fluid, *Appl. Math. Mech.* 33 (10) (2012) 1301–1312.
4. S.Pramanik, Casson fluid flow and heat transfer past an exponentially porous stretching surface in presence of thermal radiation, *Ain Shams Engineering Journal*, Volume 5, Issue 1, March 2014, Pages 205-212
5. M. Gnaneswara Reddy, Unsteady radiative-convective boundary layer flow of a Casson fluid with variable thermal conductivity, *J. Eng. Phys. Thermo Phys.* 88 (1) (2015) 240–251.
6. A. Khalid, I. Khan, S. Shafiel, Exact solutions for unsteady free convection flow of a Casson fluid over an oscillating vertical plate with constant wall temperature, *Abstr. Appl. Anal.* (15) (2015) 946350 <<http://dx.doi.org/10.1155/2015/946350>>.
7. N. Akbar, Influence of magnetic field on peristaltic flow of a Casson fluid in an asymmetric channel: application in crude oil refinement, *J. Magnet. Magnet. Mater.* 378 (2015) 463–468.
8. A. Khalid, I. Khan, A. Khan, S. Shafie, Unsteady MHD free convection flow of Casson fluid past over an oscillating vertical plate embedded in a porous medium, *Eng. Sci. Technol. Int. J.* (2015) doi:10.1016/j.jestch.2014.12.006.
9. C.S.K. Raju, N. Sandeep , V. Sugunamma, M. Jayachandra Babu, J.V. Ramana Reddy, Heat and mass transfer in magnetohydrodynamic Casson fluid over an exponentially permeable stretching surface, *Engineering Science and Technology, an International Journal* 19(2016), 45-52
10. P. BalaAnkiReddy, Magnetohydrodynamic flow of a Casson fluid over an exponentially inclined permeable stretching surface with thermal radiation and chemical reaction *Ain Shams Engineering Journal* Volume 7, Issue 2, June 2016, Pages 593-602
11. Raju, C. S. K., Sandeep, N., Sugunamma, V., Babu, M. J., & Reddy, J. R. [2016] "Heat and mass transfer in magnetohydrodynamic Casson fluid over an exponentially permeable stretching surface", *Engineering Science and Technology, an International Journal*, Vol. 19, Issue. 1, pp. 45-52.

12. Reddy, R. C., Reddy, K. J., & Ramakrishna, K. (2016). Effects of joule heating on MHD free convective flow along a moving vertical plate in porous medium. *Special Topics and Reviews in Porous Media*, 7(2), 207-219. doi:10.1615/SpecialTopicsRevPorousMedia.2016017247
13. Reddy, G. V. R. (2016). Soret and Dufour effects on MHD free convective flow past a vertical porous plate in the presence of heat generation. *International Journal of Applied Mechanics and Engineering*, 21(3), 649-665. doi:10.1515/ijame-2016-0039
14. Mangathai, P., Ramana Reddy, G. V., & Rami Reddy, B. (2016). MHD free convective flow past a vertical porous plate in the presence of radiation and heat generation. *International Journal of Chemical Sciences*, 14(3), 1577-1597.
15. Ramana Reddy, G. V., Bhaskar Reddy, N., & Chamkha, A. J. (2016). MHD mixed convection oscillatory flow over a vertical surface in a porous medium with chemical reaction and thermal radiation. *Journal of Applied Fluid Mechanics*, 9(3), 1221-1229.
16. Ramana Reddy, G. V., Bhaskar Reddy, N., & Gorla, R. S. R. (2016). Radiation and chemical reaction effects on MHD flow along a moving vertical porous plate. *International Journal of Applied Mechanics and Engineering*, 21(1), 157-168. doi:10.1515/ijame-2016-0010
17. P. Suresh, Y. Hari Krishna, R. Sreedhar Rao, P. V. Janardhana Reddy; "Effect of Chemical Reaction and Radiation on MHD Flow along a moving Vertical Porous Plate with Heat Source and Suction", *International Journal of Applied Engineering Research*, 14(4), 869-876, 2019
18. BalajiPrakash, G; Reddy, GV Ramana; Sridhar, W; Krishna, Y Hari; Mahaboob, B; Thermal Radiation and Heat Source Effects on MHD Casson Fluid over an Oscillating Vertical Porous Plate, *Journal of Computer and Mathematical Sciences*, 10(5), 1021-1031, 2019
19. P. Suresh, Y. Hari Krishna, Mahaboob, Amaranath: Heat Transfer and Stagnation Heat Stagnation-Point Flow of Non-Point Non-Newtonian Casson Fluid over Stretching Surface Fluid Surface, *International Journal of Modern Engineering and Research Technology*, Volume 6 | Issue 2 | April 2019, 33-39
20. N Vijaya, Y Hari Krishna, K Kalyani, GVR Reddy Non-Aligned Stagnation Point Flow of a Casson Fluid past a Stretching Sheet in a Doubly Stratified Medium, « *Fluid Dynamics & Materials Processing*, vol.15, no.3, pp.233-251, 2019
21. M M Hasan. "Casson Fluid Flow and Heat Transfer over a Permeable Vertical Stretching Surface with Magnetic Field and Thermal Radiation." *IOSR Journal of Engineering (IOSRJEN)*, vol. 09, no. 01, 2019, pp. 14-19.
22. O. D. Makinde, MHD mixed-convection interaction with thermal radiation and nth order chemical reaction past a vertical porous plate embedded in a porous medium, *Chemical Engineering Communications*, Volume 198, 2010 - Issue 4
23. O. D. Makinde, "MHD steady flow and heat transfer on the sliding plate," *AMSE, Modeling, Measure. Control B*, vol. 70, no. 1, pp. 61-70, 2001.
24. S. Y. Ibrahim and O. D. Makinde, "Radiation effect on chemically reacting magnetohydrodynamics (MHD) boundary layer flow of heat and mass transfer through a porous vertical flat plate," *International Journal of Physical Sciences*, vol. 6, no. 6, pp. 1508-1516, 2011.
25. O. D. Makinde, "Free convection flow with thermal radiation and mass transfer past a moving vertical porous plate," *International Communications in Heat and Mass Transfer*, vol. 32, no. 10, pp. 1411-1419, 2005.

26. O. D. Makinde and A. Ogulu, "The effect of thermal radiation on the heat and mass transfer flow of a variable viscosity fluid past a vertical porous plate permeated by a transverse magnetic field," *Chemical Engineering Communications*, vol. 195, no. 12, pp. 1575–1584, 2008.